International Journal for Innovative Engineering and Management Research
A Peer Revieved Open Access International Journal
www.ijiemr.org

COPY RIGHT

ELSEVIER
SSRN

IJIEMR Transactions, online available on 4th Jan 2019. Link :

http://www.ijiemr.org/main/index.php?vol=Volume-08&issue=ISSUE-01

Title: **NEW INCORPORATED STAGGERED CONVERTER FOR EXCHANGED HESITANCE ENGINE DRIVES IN MODULE CROSS BREED ELECTRIC VEHICLES WITH ADAPTABLE VITALITY CHANGE**

Volume 08, Issue 01, Pages: 60–83.

Paper Authors

G.KIRAN, MUKKAMLA MAHESH
Nova College Of Engineering &Technology

USE THIS BARCODE TO ACCESS YOUR ONLINE PAPER

To Secure Your Paper As Per UGC Guidelines We Are Providing A Electronic Bar Code

International Journal for Innovative Engineering and Management Research
A Peer Revieved Open Access International Journal
www.ijiemr.org

NEW INCORPORATED STAGGERED CONVERTER FOR EXCHANGED HESITANCE ENGINE DRIVES IN MODULE CROSS BREED ELECTRIC VEHICLES WITH ADAPTABLE VITALITY CHANGE

[1] G.KIRAN, [2] MUKKAMLA MAHESH
[1] Assistant Professor Nova College Of Engineering &Technology
[2] Power Electronics (M.Tech), Nova College Of Engineering &Technology

ABSTRACT:
This paper introduces a coordinated staggered converter of exchanged hesitance engines (SRMs) bolstered by a secluded front-end circuit for module cross breed electric vehicle (PHEV) applications. A few working modes can be accomplished by changing the on-off conditions of the switches in the front-end circuit. In generator driving mode, the battery bank is utilized to hoist the stage voltage for quick excitation and demagnetization. In battery driving mode, the converter is reconfigured as a four-level converter, and the capacitor is utilized as an extra charge capacitor to create staggered voltage yields, which upgrades the torque ability. The working methods of the proposed drive are clarified and the stage current and voltage are broke down in points of interest. The battery charging is normally accomplished by the demagnetization current in motoring mode and by the regenerative current in braking mode. Also, the battery can be charged by the outside air conditioning source or generator through the proposed converter when the vehicle is in halt condition. The SRM-based PHEV can work at various speeds by organizing the power stream between the generator and battery. Reenactment in MATLAB/Simulink and examinations on a three-stage 12/8 SRM affirm the viability of the proposed converter topology.
Record Terms—Quick excitation and demagnetization, front-end circuit, staggered voltage, adaptable battery charging, module half breed electric vehicle (PHEV), exchanged hesitance engine (SRM).

1. INTRODUCTION

Throughout the decades, electrified vehicles (EVs) have pulled in expanding consideration because of the fast consumption of petroleum product assets and expanding fumes gas outflows in urban situations. As a trade off of unadulterated battery-fueled and inside burning motor (ICE)- based vehicles, half breed Electric vehicles (HEVs) and module HEVs (PHEVs) give much guarantee and greater adaptability. For HEV or PHEV applications, perpetual magnet synchronous engines (PMSMs) are a prominent engine drive innovation yet their magnets normally use uncommon earth materials, which confines their boundless application in large scale manufacturing market. Therefore,

elective advances have been requested for uncommon without earth or uncommon earth-less arrangements. Exchanged hesitance engines (SRMs) are known to have a less complex and more tough development with no rotor windings and lasting magnets. They can give a more drawn out administration time in cruel situations and a more financially savvy engine drive choice than PMSMs. Also, attributable to promote inborn points of interest including high productivity, high dependability, great adaptation to non-critical failure capacity, and high beginning torque in introductory increasing speeds. SRMs are thought to be an aggressive contender for HEV and PHEV electric impetuses. Keeping in mind the end goal to enhance the SRM framework unwavering quality, position sensor less control techniques and adaptation to internal failure plans are created for wellbeing basic applications. To diminish the SRM torque swell, new direct torque control plans have been proposed to manage this issue. Besides, some cutting edge advances have been proposed to enhance the engine proficiency and relieve the vibration for car applications. Be that as it may, the incorporated SRM converter topology with numerous capacities for PHEV applications has not been created. When all is said in done, a reduced and dependable inverter/converter is required for electric vehicle footing drives. There have been some new converter topologies in light of SRMs. A novel three-stage SRM drive with charging capacities, including an ICE and a framework charging is displayed in . In any case, the quick excitation and quick demagnetization cant be accomplished, and this converter is gotten from a C-dump converter, which has no adaptation to non-critical failure capacity due to non-secluded stages in the converter circuit. In a dc/dc converter is utilized for SRM drives, and a voltage-help controller is intended to upgrade the SRM winding current and speed dynamic reactions. Ordinarily, dc/dc converters contain inductors and capacitors and in this way diminish the power thickness. A driving/accusing SRM drive of adjusted Miller converter by utilizing three-stage wise power modules is exhibited in for unadulterated battery-fueled vehicle applications, however it isnt outfitted with adaptation to non-critical failure capacity. In a SRM drive made out of a lopsided extension converter and a bidirectional front-end dc/dc converter is created for adaptable battery charging and releasing. The control plans are likewise created with brilliant quickening, deceleration and regenerative braking qualities. To acknowledge adaptable accusing elements of both dc and air conditioning sources, a four-stage SRM drive nourished by a split converter is planned in for EV applications. The four stage windings are part and their midpoints are hauled out to associate for the new converter. Be that as it may, staggered voltage cant be accomplished in motoring conditions, making it inadmissible for three-stage engine drive applications. A novel detached lift control converter for SRM is proposed in which adds an inactive circuit to the front-end of an ordinary topsy-turvy converter to support the dc-interface voltage for a high negative inclination in the demagnetization mode. Keeping in mind the end goal to get a quick current development

and appropriate demagnetization, the power converter with the capacity of expanded voltage are outlined by utilizing an extra capacitor for fast tasks. In a SRM converter with just a single switch for each stage is fit for giving a high demagnetization voltage so to build the yield torque of engine drive. In any case, it is intended for ease applications and cant accomplish quick excitation. To diminish the present rising and falling occasions, a quasithree-level converter for SRM drives is produced in . This converter needs twice the same number of intensity switches as traditional converters, which significantly increment the cost and many-sided quality of the engine drive. Another double voltage drive for SRMs is displayed in . It enables a SRM to work from air conditioning mains or a low-voltage battery supply, without a transformer to coordinate the two voltage levels. Another ease battery fueled SRM drive with driving and charging capacities is additionally proposed in . Its battery charging is specifically accomplished through the engine windings without outside transformers or other charging units. Builds up another incorporated staggered converter of SRM nourished by a measured front-end circuit for PHEV applications. By controlling the on-off conditions of the switches in the front-end circuit, differing working modes are accomplished. In generator driving mode, the stage voltage is hoisted by the battery bank for quick excitation and demagnetization. In battery driving mode, the converter is reconfigured as a four-level converter, and the quick excitation and demagnetization are likewise accomplished by the extra charge capacitor. The torque ability is elevated because of the staggered voltage. The battery is effectively charged in motoring and braking activities. In addition, the battery charging can be adaptably accomplished in stop conditions. The vitality transformation between the generator, battery bank, outer AC source and footing engine is adaptably accomplished by controlling the exchanging gadgets in the drive circuit. Contrasted with the current plans, the fundamental commitments and favorable circumstances of the paper are:

1) A coordinated staggered converter for PHEV applications is created by utilizing a less difficult front-end circuit (less power gadgets and less complex control calculation);

2) Modularized structure makes the proposed framework more minimal and reasonable for the objective pplications. The proposed converter is made out of eight topsy-turvy half extension arms and each scaffold arm contains an IGBT and a diode. For industry applications, the modularized structure is anything but difficult to fabricate and supplant. The proposed converter incorporates the generator and battery manage an account with just two IGBTs and two diodes with no additional capacitor or inductor. Accordingly, the proposed converter is more conservative with a superior power thickness. It can be extended for higher power applications and multi-stage SRMs.

3) Multiple capacities and working modes are accomplished by the proposed converter topology;

4) Excitation and demagnetization are quickened without expanding torque swells;

International Journal for Innovative Engineering and Management Research
A Peer Revieved Open Access International Journal
www.ijiemr.org

5) Drive framework effectiveness is enhanced by 2 %~4 %. The reproduction and investigations did on a three-stage 12/8 SRM approve the adequacy and points of interest of the proposed drive by applying the front-end circuit. This paper is composed as takes after: In Section II, the working guideline of SRM drives is broke down in detail. In Section III, acoordinated staggered converter for SRM-based PHEV footing drives are proposed; the working modes and the current and voltage are broke down appropriately; the favorable circumstances by applying the front-end circuit are introduced. The reenactment results in Section IV and exploratory outcomes in Section V are introduced for the confirmation of-idea of this new drive. At last, conclusions are given in Section VI.

1.1 INTRODUCTION TO SRM

This Deals with the history, development, working rule, task, recurrence variety of inductance, empowerment plan and numerical demonstrating of Switched Reluctance Motor (SRM). Moreover, different converter topologies, rotor position sensor, control parts of SRM, points of interest, disservices and applications are additionally examined. The itemized writing study of the reference papers and the issues distinguished in light of the writing study are likewise introduced in this section. Electrical drives assume an imperative part in present day businesses. Over the most recent two decades, another sort of electrical drive named the SRM drive has been presented and is nearly observed. The SRM drive has now achieved a level of development that it permits to be utilized in industry as a proficient brushless drive with the cost favorable circumstances, a wide speed extend and an intrinsic effortlessness and roughness. Be that as it may, the SRM is definitely not another idea in light of the fact that early innovators of electromagnetic motors comprehended the SRM rule, yet were unsuccessful in their endeavors to manufacture a motor attributable to its poor electromagnetic and mechanical outlines and the inaccessibility of reasonable exchanging gadgets. An enthusiasm for switched field machines was restored in the 1960s with the coming of the Thyristors. In the mid 1980s, the main SRM drive framework utilizing the new innovation turned out to be monetarily accessible because of work done by a gathering at Leeds and Nottingham Universities in the U.K. Lately, this machine has demonstrated a recovery of enthusiasm for applications in 10 W and medium power drives. Such a machine is rising 2 as an alluring answer for variable speed applications because of a few points of interest. Most noticeable among these are, the basic structure of the motor with curls on the stator and no windings or brushes on the rotor.

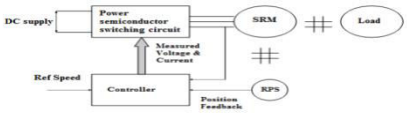

Figure 2.1.1 Block diagram of SRM

1.1.1 Block diagram of SRM

Figure 2.1.1 demonstrates the square graph of SRM. DC supply is given to the power semiconductor exchanging circuit, which is associated with different stage windings of SRM. The RPS, which is mounted on a pole of the SRM, gives signs to the controller about the situation of the rotor regarding the reference hub. The controller gathers this

International Journal for Innovative Engineering and Management Research
A Peer Revieved Open Access International Journal
www.ijiemr.org

data and furthermore the reference speed flag and reasonably kills on and the concerned power semiconductor gadgets of exchanging circuit, with the end goal that the coveted stage winding is associated with the DC supply. The present flag is additionally a nourished back to the controller circuit to confine the motor current inside allowable breaking points.

1.1.2 PRINCIPLE OF OPERATION OF SRM :

Stator posts An, An and rotor shafts a,c are in arrangement and they are in a base reluctance position so far as stage An is concerned, i.e. at this position the inductance of B stage winding is neither most extreme nor least as appeared in Figure 2.1.3

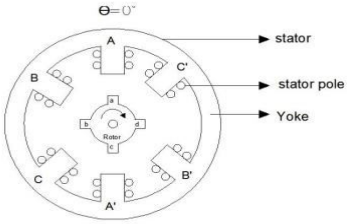

Figure 2.1.3 Basic structure of three phase 6/4 SRM

The motor builds up a torque, which is called as electromagnetic torque that is equivalent to and the course of the torque is to such an extent that B, B and b,d attempt to get an arrangement. On the off chance that this torque is more than the restricting burden and the frictional torque, the rotor starts to turn. At the point when the pole involves the position to such an extent that B,B and b,d are in arrangement, at that point no torque is created in light of the fact that is zero. Presently the stage winding B is switched off and the stage winding C is associated with DC supply. The heap encounters a torque as exists, at that point the electromagnetic torque is produced . The motor keeps on pivoting. At the point when the rotor moves encourage 30º, the torque because of C windings is zero. The motor is switched off and the stage winding An is stimulated. This is a consistent and cyclic process. As the speed builds, the heap torque necessity likewise changes and it happens when the created normal torque is more than the heap torque. The rotor achieves a dynamic harmony condition otherwise called an unfaltering state condition when the created torque is equivalent to the heap torque. In this relentless state condition, the power drawn from the mains is equivalent to the time rate of progress of vitality put away in an attractive field. At the point when the heap is expanded, the speed of the motor tends to fall, in such a situation, the power adjust is kept up and the torque created is to be expanded by expanding the current. More power is drawn from the mains and happens the other way around at whatever point the heap is lessened.

1.1.3 FREQUENCY VARAIATION OF INDUCTANCE OF SRM :

Let the quantity of striking shafts of rotor. The stator post pivot is lined up with the rotor shaft hub; accordingly the inductance is amplified. On the off chance that the stator post pivot is in uncommitted position; the inductance of the curl is limited. In one unrest of the rotor, the inductance of the stator stage winding experiences cycles of variety. Recurrence variety of the inductance of stage winding is equivalent to No. of cycles every seconds. Where N is the speed in RPM. The accompanying suppositions are made to have an extensive variety in the

International Journal for Innovative Engineering and Management Research
A Peer Revieved Open Access International Journal
www.ijiemr.org

stage twisting inductances of the stator as for rotor position, the bury polar curve of the rotor is influenced higher than the stator to post circular segment

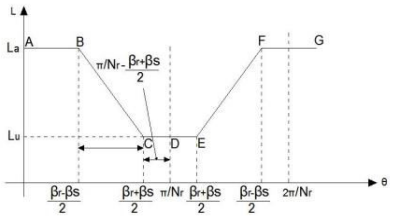

Figure 2.1.4 Frequency variation of the inductance of each phase winding of SRM

1.1.4 SHAFT POSITION SENSOR:

The motor stages ought to be energized at the rotor edges dictated by the control technique with the goal that controlling of the SRM can be performed 12 adequately. Thus, it is fundamental to have the information of the rotor position. The rotor edge data must be precise to have high determination to take into account the execution of more modern nonlinear control plots that can limit the torque swell and furthermore upgrades the motor execution. The execution of the SRM drive relies upon the exact position detecting. The proficiency of the drive and its torque yield gets diminished incredibly, by an erroneous position detecting and relating incorrect excitation edges. Give us a chance to consider an occasion where at high motor speeds, a blunder of just 1o may diminish the torque creation by very nearly 8 % of the most extreme torque yield. Customarily, rotor position data is estimated utilizing some type of mechanical edge transducer or encoder. The prerequisites of position detecting of SRM are like that of the brushless DC motor. The electromechanical sensors experience the ill effects of the accompanying impediments: *f* Due to some ecological factors, for example, high temperature, moistness, residue and vibration, these position sensors tend to be questionable. *f* For elite control, high determination encoder with staggering expense should be utilized. The cost of the sensor increments with the position determination. *f* Due to the establishment of sensor on the motor shaft, there might be an extra assembling cost and bother. *f* Proper upkeep ought to be given to the motor due to mechanical mounting of sensors, which may likewise expand the outline time and cost. 13 *f* The mechanical position sensor involves an additional electrical associations with the motor. In this way the amount of electrical wiring increments between the motor drive and motor. Therefore, it adds further to the cost of the drive framework as the wire typically should be protected from electromagnetic commotion. *f* For littler applications, the space distribution for mounting the position sensor may cause issues. Various strategies have been produced by the specialists to conquer the issues caused by the RPS and furthermore to dispense with the electromechanical sensors for determining the position data. Thus, the rotor position is resolved in a roundabout way by sensor less rotor position estimation strategies. Besides, the term sensor less infers that there are no sensors utilized. With a specific end goal to quantify the rotor position some type of sensors ought to be utilized. Essentially, the sensor less position estimation infers that there is no extra necessity of sensors to decide the position separated from those which measure the electrical parameter, for example, current or

International Journal for Innovative Engineering and Management Research
A Peer Revieved Open Access International Journal
www.ijiemr.org

voltage estimating circuits to control the motor. All the sensorless position estimation strategies for the SRM utilize some type of preparing on electrical waveforms of the motor winding. In sensorless position finder, there is no mechanical association of sensors to the motor shaft. This is the significant distinction between the sensorless position locator and electromechanical sensors. The pictorial portrayal of photograph transistor sensor is appeared in Figure 2.1.5

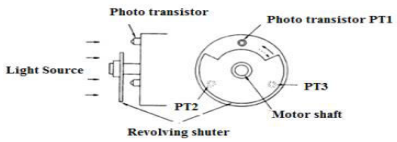

Figure 2.1.5.1 Photo transistor sensors

On the rotor shaft of SRM, a spinning screen is mounted. The screen has an electrical edge hole of 120 degrees. The quantity of photograph transistor and motor stages are equivalent and the photograph transistor is set on the stator. The photograph transistor PT1 will produce current when the hole gets lined up with it because of the episode of light. At this capacity, PT2 and PT3 have just little spillage streams on the grounds that the light is hindered by the rotating shade. Amid this stage, the stator stage related with PT1 ought to be turned on. A similar procedure will happen when the hole of spinning screen is lined up with PT2 or PT3. 1.6.1.2 Hall sensor The lobby position sensor takes a shot at the premise of the physical guideline of the corridor impact named after E.H. Corridor. It implies that if an attractive field is connected opposite to the transmitter, a voltage is created transversely 15 to the bearing of current stream in an electric channel. The diagrammatic portrayal of lobby position sensor for three stages SRM is appeared in Figure 2.1.5.2

.

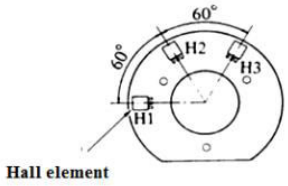

Figure 2.1.5.2 Hall position sensors

It comprises of three Hall segments and a pivoting plate with a perpetual magnet settled to the rotor shaft. The lasting magnet on the turning plate is introduced appropriately, so the yield of the corridor parts can show the best possible rotor position of the stage current control.

2. RESEARCH WORK

MULTILEVEL CONVERTER

2.1 INVERTER:

An inverter is an electrical device that devotees organize current (DC) to substituting current (AC); the changed over AC can be at any required voltage and repeat with the usage of appropriate transformers, trading, and control circuits.

Static inverters have no moving parts and are used in a broad assortment of employments, from small trading power supplies in PCs, to far reaching electric utility high-voltage facilitate current applications that vehicle mass power. Inverters are for the most part used to supply AC control from DC sources, for instance, sun arranged sheets or batteries.

The electrical inverter is a high-control electronic oscillator. It is so named in light of the way that early mechanical AC to DC converters was made to work in reverse, and

International Journal for Innovative Engineering and Management Research
A Peer Revieved Open Access International Journal
www.ijiemr.org

thusly were agitated, to change over DC to AC.

The inverter plays out the opposite limit of a rectifier.

2.1.1 CASCADED H-BRIDGES INVERTER

A solitary stage structure of a m-level fell inverter is portrayed in Figure 3.1.1.1 Each unique dc source (SDCS) is related with a single stage full-augmentation, or H-interface, inverter. Each inverter level can make three different voltage yields, +Vdc, 0, and – Vdc by partner the dc source to the aeration and cooling system yield by different blends of the four switches, S1, S2, S3, and S4. To gain +Vdc, switches S1 and S4 are turned on, while – Vdc can be gotten by turning on switches S2 and S3. By turning on S1 and S2 or S3 and S4, the yield voltage is 0. The ventilation system yields of each one of the various full-interface inverter levels are related in game plan with the ultimate objective that the mixed voltage waveform is the total of the inverter yields. The amount of yield arrange voltage levels m in a course inverter is described by m = 2s+1, where s is the amount of free dc sources. A delineation arrange voltage waveform for a 11-level fell H-interface inverter with 5 SDCSs and 5 full augmentations is showed up in Figure 3.1.1.2. The stage voltage van = va1 + va2 + va3 + va4 + va5.

For a wandered waveform, for instance, the one depicted in Figure 3.1.1.2 with s steps, the Fourier Transform for this waveform takes after

$$V(\omega t)=\frac{4V_{dc}}{\pi}\sum_{n}\left[\cos(n\theta_1)+\cos(n\theta_2)+\ldots+\cos(n\theta_s)\right]\frac{\sin(n\omega t)}{n}, \quad \text{where } n = 1, 3, 5, 7, \ldots$$

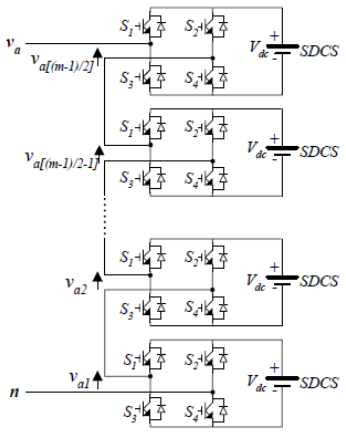

Figure 3.1.1.1Single-phase structure of a multilevel cascaded H-bridges inverter

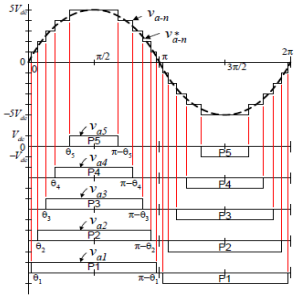

Figure 3.1.1.2 Output phase voltage waveform of an 11-level cascade inverter with 5 separate dc sources.

The magnitudes of the Fourier coefficients when normalized with respect to V_{dc} are as follows:

$$H(n)=\frac{4}{\pi n}\left[\cos(n\theta_1)+\cos(n\theta_2)+\ldots+\cos(n\theta_s)\right], \quad \text{where } n = 1, 3, 5, 7, \ldots$$

The coordinating edges, θ1, θ2, ..., θs, can be picked with the ultimate objective that the voltage indicate symphonious mutilation is a base. All things considered, these edges are picked with the objective that mind-boggling lower repeat sounds, fifth, seventh, eleventh, and thirteenth, music are shed. More detail on consonant transfer techniques will be presented in the accompanying fragment.

International Journal for Innovative Engineering and Management Research
A Peer Revieved Open Access International Journal
www.ijiemr.org

Stunned fell inverters have been proposed for such applications as static var age, an interface with reasonable power sources, and for battery-based applications. Three-arrange fell inverters can be related in wye, as showed up in Figure, or in delta. Peng has demonstrated a model stunned fell static var generator related in parallel with the electrical system that could supply or draw open current from an electrical structure.

The inverter could be controlled to either deal with the power factor of the current drawn from the source or the vehicle voltage of the electrical system where the inverter was related. Peng and Joos have moreover exhibited that a course inverter can be particularly related in game plan with the electrical system for static var pay. Fell inverters are ideal for partner maintainable power sources with an aeration and cooling system network, in light of the necessity for divided dc sources, which is the circumstance in applications, for instance, photovoltaics or vitality segments.

Fell inverters have moreover been proposed for use as the guideline balance drive in electric vehicles, where a couple of batteries or ultra-capacitors are fitting to fill in as SDCSs. The fell inverter could in like manner fill in as a rectifier/charger for the batteries of an electric vehicle while the vehicle was related with a ventilation system supply as showed up in Figure. Likewise, the course inverter can go about as a rectifier in a vehicle that usages regenerative braking.

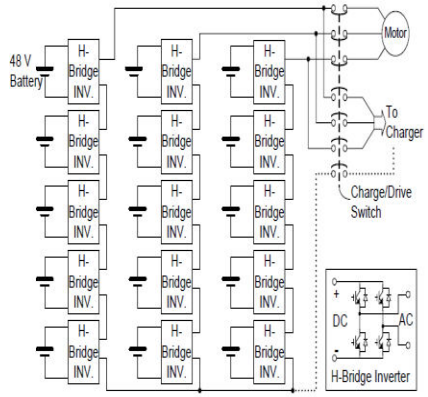

Figure 3.1.1.3 Three-phase wye-connection structure for electric vehicle motor drive and battery charging.

The essential inclinations and hindrances of amazed fell H-interface converters are according to the accompanying

Points of interest

•The number of possible yield voltage levels is more than twofold the amount of dc sources (m = 2s + 1).

•The course of action of H-ranges makes for modularized configuration and packaging. This will enable the gathering technique to be expert more quickly and productively.

Inconveniences

•Separate dc sources are required for each one of the H-ranges. This will control its application to things that starting at now have different SDCSs instantly available.

3.1.2 DIODE-CLAMPED MULTILEVEL INVERTER

The neutral point converter proposed by Nabae, Takahashi, and Akagi in 1981 was fundamentally a three-level diode-cut inverter. In the 1990s a couple of researchers conveyed articles that have reported preliminary outcomes for four-, five-, and six-level diode-cut converters for such uses as static var compensation, variable speed engine drives, and high-voltage structure interconnections. A three-organize six-level

International Journal for Innovative Engineering and Management Research
A Peer Revieved Open Access International Journal
www.ijiemr.org

diode-cut inverter is showed up in Figure. Each one of the three times of the inverter shares a run of the mill dc transport, which has been subdivided by five capacitors into six levels. The voltage over each capacitor is Vdc, and the voltage stress over each trading device is limited to Vdc through the securing diodes. Table records the yield voltage levels serviceable for one time of the inverter with the negative dc rail voltage V0 as a wellspring of viewpoint. State condition 1 suggests the switch is on, and 0 infers the turn is off. Each stage has five necessary change matches to such a degree, to the point that turning on one of the switches of the consolidate requires that the other correlative turn be slaughtered. The correlative switch sets for organize leg an are (Sa1, Sa1), (Sa2, Sa2), (Sa3, Sa3), (Sa4, Sa4), and (Sa5, Sa5). Table moreover exhibits that in a diode-cut inverter, the switches that are on for a particular stage leg are always abutting and in course of action. For a six-level inverter, a course of action of five switches is on at any given time.

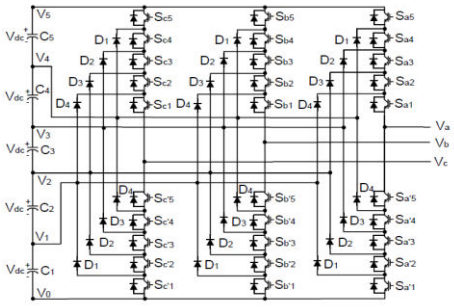

Figure 3.1.2 Three-phase six-level structure of a diode-clamped inverter.

Diode-clamped six-level inverter voltage levels and corresponding switch states.

Voltage V_{a0}	Switch State									
	S_{a5}	S_{a4}	S_{a3}	S_{a2}	S_{a1}	$S_{a'5}$	$S_{a'4}$	$S_{a'3}$	$S_{a'2}$	$S_{a'1}$
$V_5 = 5Vdc$	1	1	1	1	1	0	0	0	0	0
$V_4 = 4Vdc$	0	1	1	1	1	1	0	0	0	0
$V_3 = 3Vdc$	0	0	1	1	1	1	1	0	0	0
$V_2 = 2Vdc$	0	0	0	1	1	1	1	1	0	0
$V_1 = Vdc$	0	0	0	0	1	1	1	1	1	0
$V_0 = 0$	0	0	0	0	0	1	1	1	1	1

Table 3.1.2 Switching State Of Three-phase six-level structure of a diode-clamped inverter

ADVANTAGES:

The majority of the stages share a regular dc transport, which confines the capacitance essentials of the converter. In this way, a back to back topology isnt simply possible yet also realistic for usages, for instance, a high-voltage successive between affiliations or an adjustable speed drive.

•The capacitors can be pre-charged as a social event.

•Efficiency is high for key repeat trading.

DISADVANTAGES:

•Real control stream is troublesome for a lone inverter in light of the fact that the widely appealing dc levels will tend to cheat or discharge without correct checking and control.

•The number of supporting diodes required is quadratic ally related to the amount of levels, which can be massive for units with a high number of levels.

3.1.3 FLYING CAPACITOR MULTILEVEL INVERTER

Maynard and Foch displayed a flying-capacitor-based inverter in 1992 [32]. The structure of this inverter resembles that of the diode-fastened inverter except for that rather than using securing diodes, the inverter uses capacitors in their place. The circuit topology of the flying capacitor amazed inverter is showed up in Figure 3.1.3. This topology has a venturing stool structure of dc side capacitors, where the

International Journal for Innovative Engineering and Management Research
A Peer Revieved Open Access International Journal
www.ijiemr.org

voltage on each capacitor contrasts from that of the accompanying capacitor. The voltage increase between two adjacent capacitor legs gives the range of the voltage wanders in the yield waveform.

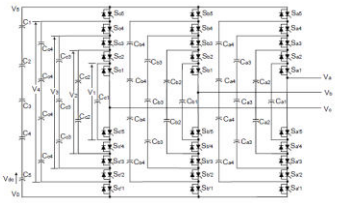

Figure 3.1.3 Three-phase six-level structure of a flying capacitor inverter.

One ideal position of the flying-capacitor-based inverter is that it has redundancies for inward voltage levels; by the days end, no less than two honest to goodness switch mixes can join a yield voltage. Not in any manner like the diode-propped inverter, does the flying-capacitor inverter not require most of the switches that are on (driving) be in a nonstop game plan.

Moreover, the flying-capacitor inverter has organize redundancies, however the diode-propped inverter has simply line-line redundancies [2, 3, 33]. These redundancies allow a choice of charging/discharging specific capacitors and can be combined in the control system for changing the voltages over the distinctive levels.

Despite the (m-1) dc interface capacitors, the m-level flying-capacitor amazed inverter will require (m-1) × (m-2)/2 aide capacitors for each stage if the voltage rating of the capacitors is vague to that of the key switches. One application proposed in the written work for the stunned flying capacitor is static var age [2, 3]. The essential purposes of intrigue and disadvantages of amazed flying capacitor converters are according to the accompanying [2, 3].

Central focuses:

•Phase redundancies are open for altering the voltage levels of the capacitors.

•Real and responsive power stream can be controlled.

•The tremendous number of capacitors engages the inverter to ride through brief length power outages and significant voltage hangs.

Obstructions:

•Control is snared to track the voltage levels for most of the capacitors. Also, restoring most of the capacitors to a comparable voltage level and startup are awesome.

•Switching use and capability are poor for bona fide control transmission.

The sweeping amounts of capacitors are both more expensive and gigantic than clamping diodes in amazed diode-caught converters. Packaging is moreover more troublesome in inverters with a high number of levels.

Plug-in Hybrid Electric Vehicles

The Chevrolet Volt is the worlds best offering module hybrid[1] Global consolidated Volt/Amper family deals A module half breed electric vehicle (PHEV) is a cross breed electric vehicle whose battery can be revived by connecting it to an outer wellspring of electric power also by its on-board motor and generator. Most PHEVs are traveler autos, yet there are additionally PHEV forms of business vehicles and vans, utility trucks, transports, trains, motorcycles, bikes, and military vehicles.

International Journal for Innovative Engineering and Management Research
A Peer Revieved Open Access International Journal
www.ijiemr.org

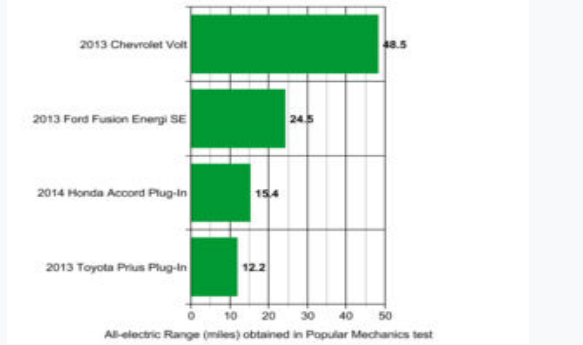

3. OPERATING PRINCIPLE OF SRM DRIVE

An ordinary hilter kilter half-connect converter is typically embraced in SRM drives because of its stage disconnection, magnificent solidness and blame tolerant capacity. With a specific end goal to lessen the torque swell and exchanging misfortune, it normally receives a delicate slashing mode in the stage turn-on area [49]. At the point when a stage winding is empowered by a positive dc-interface voltage, this stage works in the excitation mode. In the demagnetization or regenerative braking mode, the stage is liable to a negative dc-interface voltage. A positive torque is created when the present leads in the inductance climbing locale and a negative torque is delivered when the current is connected in the inductance plummeting district. The electromagnetic torque bearing can be straightforwardly controlled by tweaking the turn-on and kill edges. At fast, a negative torque is produced because of the demagnetization current in the inductance plunging area, which corrupts the motoring execution. Be that as it may, there can be no negative torque when the demagnetization voltage is expanded and the kill point can be set slacked to build the successful current territory for yield torque improving. Fig. 4.1 demonstrates the square outline of a speed-controlled SRM drive by utilizing a present direction plot. The present reference is handled through an edge rationale obstruct with a hysteresis band △ I, to acquire the imax (I *+△ I) and imin (I * - △ I) to decide the exchanging states in the stage turn-on locale. The motor speed is acquired from a speed adding machine by distinguishing the rotor position with a position sensor. The speed blunder is prepared however a speed controller, for example, a relative essential (PI) controller, to give the present reference for direction. The turn-on and kill edges, θon and θoff, are dictated by the rotor position to control the stage recompense.

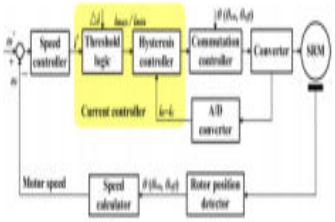

Fig. 4.1 Block diagram of the speed-controlled SRM system

4. PROPOSED INTEGRATED MULTILEVEL CONVERTER FOR PHEVS

A. Proposed Integrated Multilevel Converter

The proposed control converter is developed with a front-end circuit and an ordinary unbalanced half-connect converter, as appeared in Fig. 5.1. The front-end circuit incorporates an air conditioner electric machine (G/M), an IGBT connect rectifier/inverter (R/I), a capacitor (C), and a battery bank (B). Additionally, a hand-off (J), two IGBTs (S01 and S02), and two diodes (D01 and D02) are utilized in blend to accomplish distinctive working modes. The IGBTs utilized in the converter are with a quick recuperation against parallel diode

International Journal for Innovative Engineering and Management Research
A Peer Revieved Open Access International Journal
www.ijiemr.org

inside. In the proposed motor drive, the battery bank B is used to interface the power wellspring of the generator to accomplish the staggered voltage for generator driving tasks, and the capacitor C is likewise used to lift the dc-connect voltage for the battery driving activities. The demagnetization streams and braking ebbs and flows can specifically input to the power supply however the counter parallel diode in the switch S01 for battery charging. Fig. 5.2 demonstrates the four working methods of the proposed converter, which can be adaptably accomplished by controlling the onoff conditions of the exchanging gadgets (S01 and S02) in the Front end circuit.

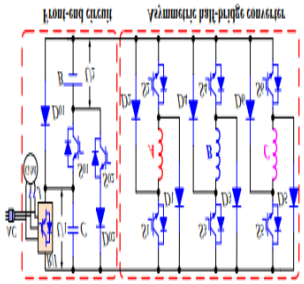

Figure 5.1Proposed Integrated Inverter Fed by Front-End Circuit

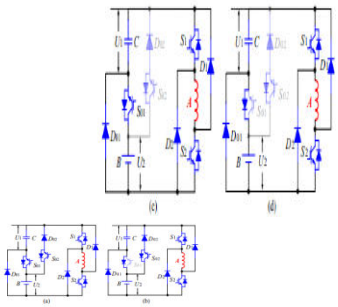

Figure 5.2 Operating Modes of the Proposed Front-End Dual-Source Circuit

(a) Model1:S01 on,S02 on
(b) Model 2 : S01 off,S02 on
(c) Model 3:S01 on,S02 off
(d) Model 4:S01 off,S02 off

B. Excitation: Mode When transfer J is on, the motor can be driven by both the generator and battery, or the single generator. In this state, Fig. 5.2(a), (b) and (d) demonstrate the excitation methods of the proposed converter under various voltage conditions. Fig. 5.2(a) demonstrates the excitation mode E1 that stage An is invigorated from the dualsource when S01 is on and S02 is off. Fig. 5.2(b) demonstrates the excitation mode E2 that stage An is invigorated from the single generator when S01 and S02 are both killed. Fig. 5.2(d) demonstrates the freewheeling mode that stage An is in a zero-voltage circle (ZVL) when S1 is off and S2 is on. At the point when hand-off J is off, and S02 is on, the motor is driven by the single battery, and the converter is reconfigured as a four-level converter . In this express, the excitation modes are appeared in Fig. 5.2(a) and (c). The capacitor C can be viewed as an extra charge capacitor contrasted with the regular unbalanced converter. At the point when S01 is on, the charged voltage of the extra capacitor is connected to the stage twisting in the excitation mode for quick current development, as appeared in Fig. 5.2(a). At the point when S01 is off, stage An is empowered from the single battery in the excitation mode E3, as appeared in Fig. 5.25(c). The demagnetization current is quickly diminished amid the energizing of the capacitor in demagnetization mode, which would lessen the negative torque from

International Journal for Innovative Engineering and Management Research
A Peer Revieved Open Access International Journal
www.ijiemr.org

the tail current in rapid activities.

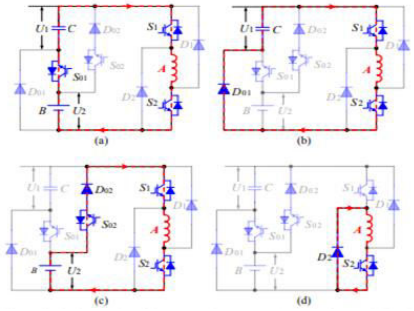

Figure 5.3 Excitation modes of the proposed converter

(A) Excitation mode E1
(B) Excitation mode E2
(C) Excitation mode E3
(D) Free Wheeling Diode

C. Demagnetization Mode and Battery Chargin: Fig. 5.3 demonstrates the demagnetization methods of stage An in the proposed converter under various voltage conditions. Fig. 5.3(a) demonstrates the two-stage current non-covering state, and Fig. 5.3(b)~(f) demonstrate the two-stage current covering states. Fig. 5.3(a) demonstrates the quick demagnetization mode D1 under the voltage of U1+U2, when stage An and stage B streams are not covered; Fig. 5.3(b) demonstrates the quick demagnetization mode D2 under the voltage of U1+U2, when stage An and stage B streams have a cover, and stage B is in the freewheeling mode in a ZVL; Fig. 5.3(c) demonstrates the quick demagnetization mode D3 under the voltage of U1+U2, when stage An and stage B streams have a cover, and stage B is invigorated from stage A; Fig. 5.3(d) demonstrates the demagnetization mode D4 when stage B is invigorated under the voltage of U1+U2, both from the double source and stage A; Fig. 5.3(e) demonstrates the demagnetization mode D5 when stage B is stimulated under the voltage of U1, both from the generator and stage A; Fig. 5.4(f) demonstrates the demagnetization mode D6 when stage B is invigorated under the voltage of U2, both from the battery and stage A. The battery is normally charged by the demagnetization current through the counter parallel diode in S01, independent of S01 being on or off, and the demagnetization voltage of stage An is U1+U2, as appeared in Fig. 5.4(a)~(c). On the off chance that the converter works in the regenerative braking task, the battery is charged by the regenerative braking current, additionally as appeared in Fig. 5.4(a)

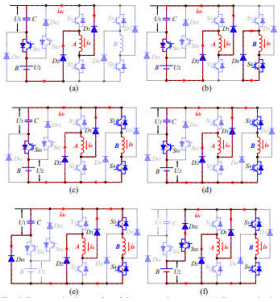

Figure 5.4 Demagnetization modes of the proposed converter

(A)Demagnetization mode D1
(B)Demagnetization mode D2
(C)Demagnetization mode D3
(D)Demagnetization mode D4
(E)Demagnetization mode D5
(F)Demagnetization mode D6

D. Investigation of Phase Current and Phase Voltage In a present period, each stage experiences three principle modes: 1) excitation mode, 2) freewheeling mode and 3) demagnetization mode. The working methods of the proposed converter encouraged by the front-end circuit are unique in relation to those of the regular converter in the stage replacement locale. Fig. 5.5 demonstrates the connection between the stage current and stage voltage

International Journal for Innovative Engineering and Management Research
A Peer Revieved Open Access International Journal
www.ijiemr.org

under various source driving modes. As appeared in Fig. 5.5(a), the stage voltage switches amongst +U1 and – U1 in the customary converter without front-end circuit; while in the proposed converter, staggered voltage is acquired and quick excitation and quick demagnetization are accomplished both in the generator and battery driving modes, as appeared in Fig. 5.5(b) and (c).

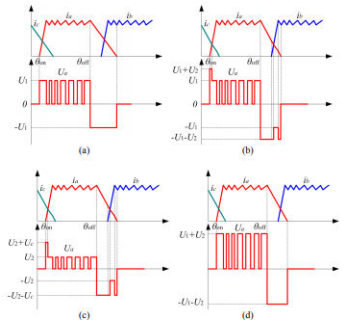

Figure 5.5 Phase current and phase voltage
(A)In conventional converter
(B)Driven by the generator in new converter
(C)Driven by the battery in new converter
(D)Driven by the dual-source in new converter

The switches S01 and S02 and hand-off J in the front-end circuit are utilized to choose the working modes including generator driving mode, battery driving mode and double source driving mode. Mode P1—Driven by the Generator: When transfer J is on and S01 and S02 are both off, the motor is driven by the single generator, and the working method of the converter is appeared in Fig. 5.5(d). The stage current and stage voltage in this condition is displayed in Fig. 5.5(b). In the covered demagnetization locale of stages An and excitation area of stage B, when the demagnetization current ia is bigger than the excitation current ib, stage A present streams to the double source and stage B to manufacture the excitation current of stage B, and at the same time charges the battery, as appeared in Fig. 5.5(c). In this mode, stage A goes about as a present source under the demagnetization voltage of the battery bank B and capacitor C. In this express, the voltage and current conditions of stage An are given by

$$U_a = -U_1 - U_2 = R_a i_a + L_a(\theta)\frac{di_a}{dt} + i_a\omega\frac{dL_a(\theta)}{d\theta}$$

$$i_a = i_{dc} + i_b$$

where Ra is the stage A winding obstruction, ia is the stage A current, θ is the rotor position, La(θ) is the stage A winding inductance, ib is the stage B current, and idc is the dc-interface current. At the point when the demagnetization current of stage An ia is littler than the excitation current of stage B ib, it isnt sufficient to fabricate the excitation current for stage B, and stage B winding is invigorated from both the generator and stage A twisting, as appeared in Fig. 5.5(e). In this mode, stage An is under the demagnetization voltage of capacitor C, and the voltage and current conditions of stage An are given by

$$U_a = -U_1 = R_a i_a + L_a(\theta)\frac{di_a}{dt} + i_a\omega\frac{dL_a(\theta)}{d\theta}$$

$$i_a = -i_{dc} + i_b$$

In the covered demagnetization district of stage An and freewheeling locale of stage B, stage A present streams back to the double source and all the while charges the battery bank, where stage B is in a ZVL, as appeared in Fig. 5.5(b). In this mode, stage An is under the demagnetization voltage of the battery bank B and capacitor C. The stage A voltage can be figured as (1), and the stage A current is equivalent to the dc-connect current. So also, in the excitation district of stage A, when the demagnetization current of stage C is bigger

International Journal for Innovative Engineering and Management Research
A Peer Revieved Open Access International Journal
www.ijiemr.org

than the excitation current of stage A, the stage C current streams to the double source and in the interim forms the excitation current of stage A. In this express, the stage A winding is stimulated from the stage C twisting under the voltage of the battery bank B and capacitor C. In the excitation area of stage A, when the demagnetization current of stage C is littler than the excitation current of stage A, the source supplies the current to stage A winding, and it is invigorated from both the generator and stage C winding. At the point when hand-off J is off and S02 is on, the motor is driven by the single battery and the converter is reconfigured as a four-level converter, and the working methods of the converter are appeared in Fig. 5.5(b). The stage current and stage voltage in this condition is exhibited in Fig. 5.5(c). This mode is like mode P1. The distinctions are that the power source is exchanged to the battery bank, and the capacitor C is revived as an extra source to raise the dc-connect voltage in the stage substitution areas. Mode P3—Driven by the Dual-Source: When hand-off J is on and S01 is on, the motor is driven by both the generator and battery, and the working method of the converter are appears in Fig. 5.5(a) or (c). The stage current and stage voltage in this condition is exhibited in Fig. 5.5(d). In both excitation and demagnetization areas of stage A, the stage voltage is the voltage of the battery bank B and capacitor C. The voltage condition of stage An are given by (1) in the demagnetization locale, and (5) in the excitation district. E. Double Source Energy Exchange When the PHEV is in halt condition, the capacitor C can change the battery bank B by controlling the power switches in the drive circuit. There are two working stages in this condition, as appeared in Fig. 5.5(a) and (b). In working stage 1, switches S1~S6 are turned on in the meantime to empower all the stage windings. In working stage 2, turns S1~S6 are killed in the meantime, and the vitality put away in the stage windings is released to the capacitor C and battery bank B however the diodes D1~D6. In this advance, the battery bank can be adaptably charged by the vitality from the capacitor. The stage current in working stage 1 can be communicated as

Generally the generator is likewise with the capacity of a starter that can begin the motor from halt. Along these lines, the battery bank needs to supply vitality to capacitor C to begin the motor, and the electric machine M/G works as a motor. In this situation, working stage 3 is required as appeared in Fig. 5.5(c), in which the battery bank invigorates the three stage windings of the motor. Uncommonly, in this condition, the capacitor voltage U1 is lower than the battery bank voltage U2 and capacitor C cant supply the vitality to stage windings. At that point, killing the exchanging gadgets S1~S6, the winding vitality is released to the capacitor and battery bank, as appeared in Fig. 5.5(b).In this advance, the battery bank vitality is exchanged to capacitor C.

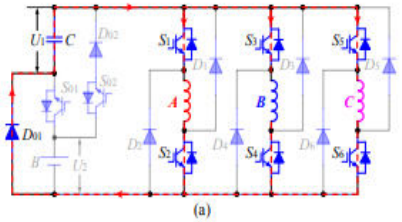

.

International Journal for Innovative Engineering and Management Research
A Peer Revieved Open Access International Journal
www.ijiemr.org

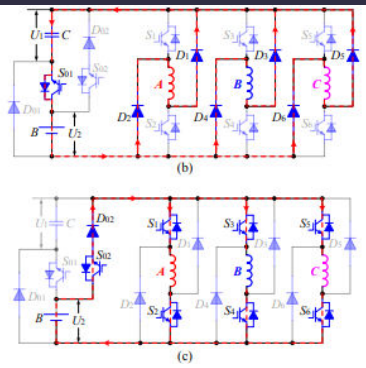

Figure 5.6Working stages of dual source energy exchange

(A)Working stage-1

(B)Working stage-2

(C)Working stage-3

E. Coordination of the Dual-Source Fig. 5.6 demonstrates the power stream between the generator, battery bank, SRM and outside AC hotspot for motoring and charging conditions, separately, where the vitality change is adaptably accomplished amid the activities. Fig. 5.7 demonstrates the coordination of the generator and battery working at various paces. The generator and battery can cooperate or freely as indicated by the speed varieties, to enhance the beginning, increasing speed and consistent state exhibitions. The staggered voltage including the quick excitation and quick demagnetization are both accomplished in generator and battery driving modes for torque

Ability enhancements.

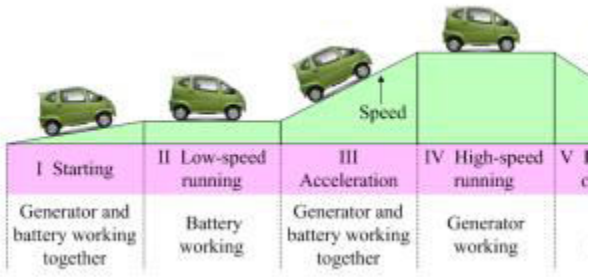

Figure5.7Coordination of the generator and the battery working in different speed conditions

F. Control Schemes for SRM Drives: The current hacking control and voltage beat control are utilized as two essential plans. As per the given speed ω* , the current slashing control is actuated at a lower speed and the voltage beat control is enacted at a higher speed, as represented in Fig. 10. The motor speed is estimated from a speed number cruncher by utilizing an encoder. The speed mistake is handled however a PI controller to manage the motor speed. The turn-on and kill edges are dictated by the position finder to control the stage replacement. In the current slashing control conspire, the stage current is tended to by a present controller. The present reference I * is gotten from the speed controller. The quick stage streams are estimated by current sensors, and sustained back to the edge rationale to figure imax and imin that decide the exchanging states in each stage turn-on district. In the voltage beat control conspire, the divert on edge is gotten from the edge controller, and managed by the prompt speed.

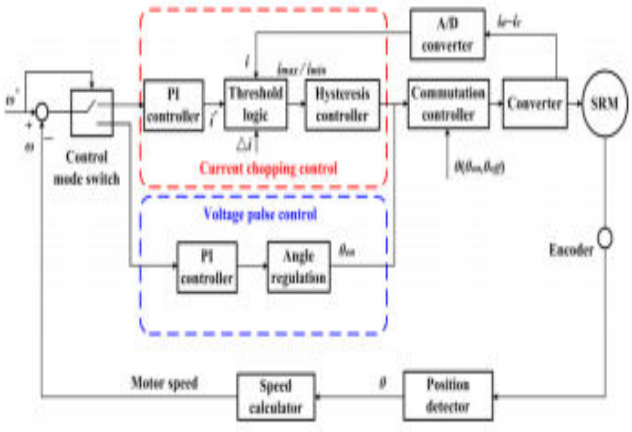

Control schemes for srm drives

International Journal for Innovative Engineering and Management Research
A Peer Revieved Open Access International Journal
www.ijiemr.org

6. SIMULATION RESULTS:

To confirm the plausibility of the proposed converter topology, a low-control three-stage 12/8-post model SRM is utilized for confirmation of-idea. The motor parameters are given in Table I. The recreation model of the motor framework is set up in MATLAB/Simulink, as appeared in Fig. 5.8. The proposed converter is built by utilizing the IGBT module with an antiparallel diode inside from SimPowerSystems. The drive signals are created from a hysteresis controller and a recompense controller, as per the given speed, rotor position and load. The momentary speed is ascertained by the heap torque and aggregate torque sent out from the motor model. The rotor position is gotten from a position mini-computer as indicated by the quick speed. Two look-into tables including the fluxcurrent-position (ψ-I-θ) and torque-current-position (T-I-θ) qualities got from the numerical electromagnetic examination by Ansoft programming are utilized to assemble the SRM demonstrate, as appeared in Fig.5.8(b).

TABLE I
MOTOR PARAMETERS

Parameters	Value
Phase number	3
Stator/rotor poles	12/8
Rated power (W)	750
Rated speed (r/min)	1500
Phase resistor (Ω)	3.01
Minimum phase inductance (mH)	27.2
Maximum phase inductance (mH)	256.7
Rotor outer diameter (mm)	55
Rotor inner diameter (mm)	30
Stator outer diameter (mm)	102.5
Stator inner diameter (mm)	55.5
Stack length (mm)	80
Stator arc angle (deg)	14
Rotor arc angle (deg)	16

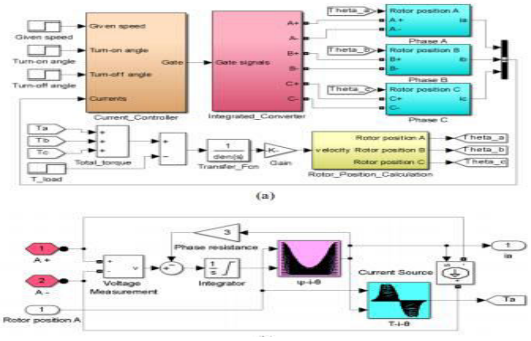

Fig. 5.8. Simulation model of the SRM drive.

(a) System model.

(b) SRM model for phase A

In the reenactments, the generator voltage and battery voltage are set to 80 V and 48 V, individually; the present hysteresis width is set to 0.1 A; the heap is set to 1.8 N·m. In the reproduction waveforms, ia, ib, and ic are the stage A, stage B, and stage C streams individually, Ua is the stage A voltage, and is the battery current. Fig. 5.9 demonstrates the stage streams, stage voltage and battery current at 300 r/min. The stage voltage and stage current in a traditional converter without front-end circuit is appeared in Fig. 5.9(a). The stage A voltage switches between +80 V and - 80V because of the exchanging states. In the proposed drive, when S01 and S02 are both off, the motor works in the generator driving mode. As showed in Fig. 5.9(b), the sit out of gear battery bank is utilized to help the stage voltage to 128 V in the substitution area to get both the quick excitation and quick demagnetization, and it is at the same time charged by the demagnetization current. Fig. 5.9(c) demonstrates the reproduction results in battery driving mode. In this state, transfer J is killed, S01 is killed and S02 is turned on, and the converter is reconfigured as a four-level converter. The capacitor C is utilized as an extra charge capacitor to lift the stage voltage both in the excitation locale for quick current development and demagnetization district for quick current exhausting. The battery bank is released in the excitation district and charged in the demagnetization locale, individually. Fig. 5.9(d) demonstrates the recreation results in dualsource driving mode when S01 is on and S02 is off.

International Journal for Innovative Engineering and Management Research
A Peer Revieved Open Access International Journal
www.ijiemr.org

(a) System demonstrate.

(b) SRM demonstrate for stage A

In the recreations, the generator voltage and battery voltage are set to 80 V and 48 V, individually; the present hysteresis width is set to 0.1 A; the heap is set to 1.8 N·m. In the reenactment waveforms, ia, ib, and ic are the stage A, stage B, and stage C streams individually, Ua is the stage A voltage, and is the battery current. Fig. 5.9 demonstrates the stage streams, stage voltage and battery current at 300 r/min. The stage voltage and stage current in a regular converter without front-end circuit is appeared in Fig. 5.9(a). The stage A voltage switches between +80 V and - 80V because of the exchanging states. In the proposed drive, when S01 and S02 are both off, the motor works in the generator driving mode. As delineated in Fig. 5.9(b), the sit out of gear battery bank is utilized to help the stage voltage to 128 V in the substitution district to get both the quick excitation and quick demagnetization, and it is all the while charged by the demagnetization current. Fig. 5.9(c) demonstrates the recreation results in battery driving mode. In this state, transfer J is killed, S01 is killed and S02 is turned on, and the converter is reconfigured as a four-level converter. The capacitor C is utilized as an extra charge capacitor to raise the stage voltage both in the excitation area for quick current development and demagnetization district for quick current exhausting. The battery bank is released in the excitation area and charged in the demagnetization district, individually. Fig. 5.9(d) demonstrates the reproduction results in dualsource driving mode when S01 is on and S02 is off.

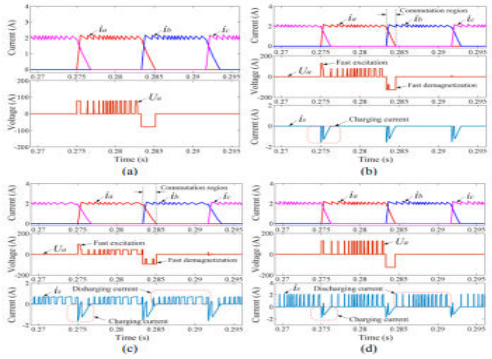

Fig.5.9.Simulation results for low-speed operation.

(A)Conventional converter.

(B)Driven by the converter.

(C)Driven by the battery.

(D)Driven by the dual source.

Fig. 5.10 shows the simulation results at 1500 r/min. The fast excitation and fast demagnetization with battery charging are also achieved in generator driving mode in high-speed operations, as shown in Fig. 5.10(a). In Fig. 5.10(b), the generator and battery bank are connected in series to drive the motor, and the battery bank is charged and discharged alternately.

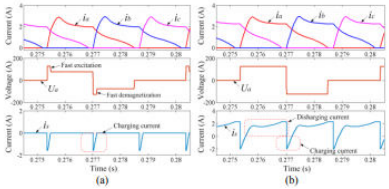

5.10 Simulation results for high speed operation

(A)Driven by the generator

(B)Driven by the dual source

At the point when the motor is in stop condition, the battery charging can be adaptably accomplished by the outer AC source or generator through the motor windings. The recreation results for battery charging in this state, where the exchanging recurrence is set to 500 Hz, and the obligation cycle is set to 0.5 and 0.6 . At the

International Journal for Innovative Engineering and Management Research
A Peer Revieved Open Access International Journal
www.ijiemr.org

point when all switches are turned on in the meantime, the three stage windings are at the same time invigorated from the outer source or generator, and the stage streams increment until the point that the switches are killed. At that point, the put away vitality in the motor windings is exchanged to the battery bank. In this advance, the battery bank can be adaptably charged by controlling the exchanging recurrence and obligation cycle.

5.2 EXPERIMENTAL RESULTS:

With a specific end goal to approve the adequacy of the proposed converter topology, a 750-W SRM is prototyped utilizing similar parameters in reenactment. The photo of the trial setup is appeared in Fig. 5.11. The motor is driven by the proposed converter with the front-end circuit. The IGBT module (IKW75N60T) with a quick recuperation hostile to parallel diode inside is utilized to develop the proposed converter topology. A movable dc control supply with 80 V is used to mimic the power source from the generator. A 48 V lead-corrosive battery bank is utilized as the vitality stockpiling gear. The rotor position is recognized by utilizing a 2500-line incremental encoder. A dsPACEDS1006 stage is utilized as the primary controller with fringe fast rationale circuits in the setup. An attractive brake is utilized to give the heap to SRM. The stage streams are recognized from the Hall-impact current sensors (LA-55P) and all the while examined by 14-bit A/D converters to execute the present control plot.

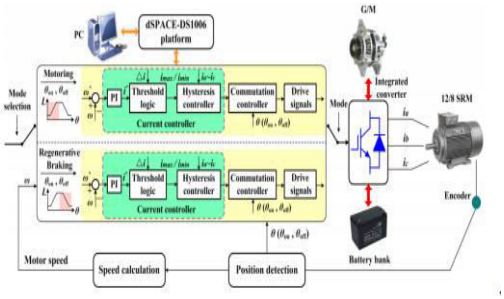

Fig. 5.11. Experimental diagram of the control system

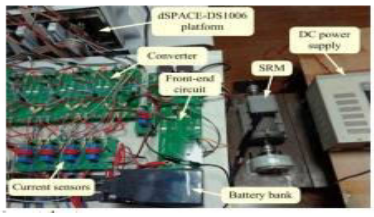

Figure. 5.12. Experimental setup

The control outline of the SRM framework inside the proposed coordinated staggered converter in motoring and braking modes is schematically represented in Fig. 5.13. The switches S01 and S02 and hand-off J in the front-end circuit are utilized to choose the working modes including generator driving mode, battery driving mode and double source driving mode. controller is utilized to manage the stage current and a PI controlle

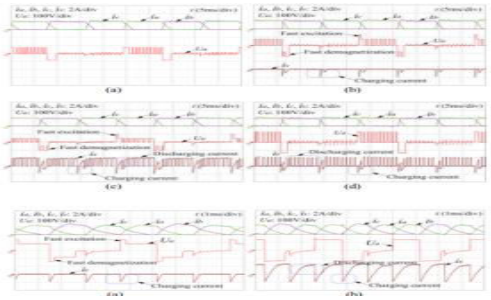

Figure 5.13 Experimental results for high speed operation

(A)Driven by the generator

(B)Driven by the dual source

The examination of the startup activity driven by the single generator and double source are exhibited in Fig. 5.14. In Fig.

International Journal for Innovative Engineering and Management Research
A Peer Revieved Open Access International Journal
www.ijiemr.org

5.14(a), the startup time is 3.5 s in single generator driving mode until the point that the speed is settled at 1500 r/min, while 1.2 s in double source driving mode, as appeared in Fig. 5.14(b). The proposed converter topology enhances the startup execution of the motor framework by utilizing double source associated in arrangement, accomplishing a quick speed reaction. The transient movement in a shut circle framework is appeared in Fig. 5.15. The motor is driven by the battery at 300 and 800 r/min, and by the generator at 1500 r/min in unfaltering state task, while driven by the double source amid increasing speed process. As appeared in Fig. 5.15(a), the immediate speed takes after the given qualities well when the motor speed ascends from 300 to 800 r/min and from 800 to 1500 r/min independent of low-speed or rapid task, in spite of speed changes amid increasing speed. At the point when the heap increments from no-heap to 1.8 N·m and 1.8 to 3.6 N·m, the speed is quickly balanced out at the given esteem, as appeared in Fig. 5.15(b). Henceforth, the created motor drive has quick reaction to the speed and load varieties. Fig. 5.16 shows test results for braking task condition. The braking time is shorter and the vitality is reused to the battery bank by utilizing the edge regulation in regenerative braking task in Fig. 5.16(b) and (c), contrasted with the inertial halting in Fig. 5.16(a). In the regenerative braking movement, the turn-on and kill edges are set to 20° and 30° in Fig. 5.16(b), and 20° and 40° in Fig. 5.16(c). The braking times are 1.8 s and 0.8 s, individually. The battery bank is charged by the regenerative current through the front-end circuit without strain and the framework acquires the fast braking capacity. The charging current and braking time can be adaptably controlled by regulating the turn-on and kill points.

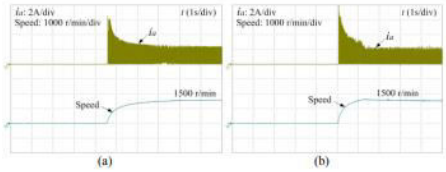

Figure 5.14Experimental results for start-up operation

(A) Driven by the single generator

(B) Driven by the dual source

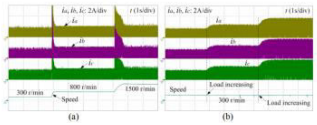

Figure 5.15 Experimental results under transient conditions

(A)Speed Increasing

(B)Load increasing

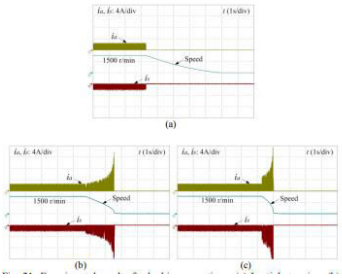

Figure 5.16 Experimental results for braking operation

(A)Inertial stopping

(B)Turn-on angle 20(degree) and turn-off angle30(degree)

(C)Turn-on-angle20(degree) and turn-off angle40(degree)

Fig. 5.17 demonstrates the charging current waveforms when the motor is in stop conditions, where PZ is the rotor encoder flag. The encoder flag keeping at zero evidences that the proposed halt charging does not cause the motor development. The exchanging recurrence is set to 500 Hz and

International Journal for Innovative Engineering and Management Research
A Peer Revieved Open Access International Journal
www.ijiemr.org

obligation cycle is set to 0.5 and 0.6, individually, in Fig. 5.17(a) and (b). Every one of the switches are turned on in the meantime to empower the three stage windings, and afterward killed in the meantime to exchange the put away vitality to the battery bank. The battery can be adaptably charged by the outer AC source or generator in this condition.

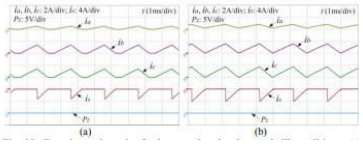

Figure 5.17 Experimental results for battery charging in stand still conditions

(A)Duty cycle 0.5

(B)Duty cycle 0.6

The current and voltage waveforms of the battery framework in running and halt conditions are appeared in Fig. 23, where Us is the battery voltage and is the charging current. A stream charging can be accomplished by the demagnetizationThe torque correlations of the proposed staggered converter with front-end circuit and the customary converter without front-end Clearly, the torque swell isnt expanded in the proposed drive in generator driving mode or battery driving mode. Fig. 26 demonstrates the effectiveness examination between the proposed and regular motor frameworks. At low speeds, the productivity of the proposed framework is somewhat higher than the ordinary one; the effectiveness is higher in fast task because of the negative torque decrease. For low-control SRM drives, their framework.

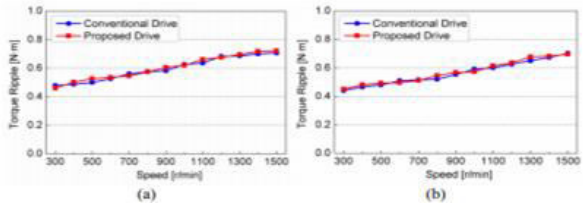

5.18 Torque comparision

(A)Generator mode

(B)Battery mode

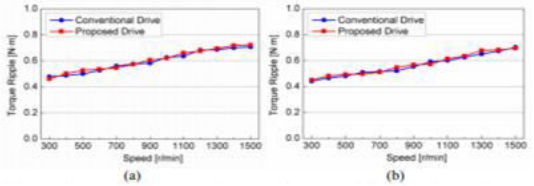

5.19Torqueripplecomparision

(A)Generator driving mode

(B)Battery driving mode

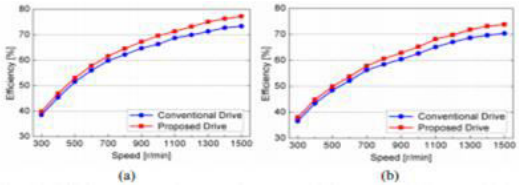

5.20 Efficiency torque comparison

(A) Generatordrivingmode

6. CONCLUSION

A new SRM drive fed by a modular front-end circuit is proposed for PHEV applications. Multimode and multilevel voltages are achieved by controlling the on-off state of the switches in the front-end circuit. The excitation modes and demagnetization modes of the proposed converter are presented, and the voltage and current in different working states are analyzed in details. Compared to the existing schemes, an improved front-end circuit is employed for multilevel voltage and multimode operations using less power devices and simpler control algorithm. The proposed topology is easy to manufacture and replace due to its modularized structure. The proposed converter integrates the

generator and battery bank in the drive system with only two IGBTs and two diodes without adding extra capacitors and inductors. Therefore, the proposed converter is more compact with a better power density. It can be expanded for higher power applications and multi-phase SRMs. The excitation and demagnetization are accelerated compared to conventional converters. The torque capability is improved by 30 % because of multilevel voltages, without increasing any torque ripples. The motor system efficiency is improved by 2 %~4 %. Moreover, the battery can be flexibly charged in standstill, motoring and braking conditions, without recourse to off-board charging facilities. The simulation and experimental tests are carried out to confirm the effectiveness of the proposed converter topology. It should be noted that this is a proof-of-concept work and the power rating is relatively low. However, the proposed SRM drive shows good scalability to build up to high-voltage and high power systems if required.

7. REFERENCES

[1] A. A. Ferreira, J. A. Pomilio, G. Spiazzi, and L. de Araujo Silva, Energy management fuzzy logic supervisory for electric vehicle power supplies system, IEEE Trans. Power Electron., vol. 23, no. 1, pp. 107-115, Jan. 2008.

[2] B. Ji, X. Song, W. Cao, V. Pickert, Y. Hu, J. W. Mackersie, and G. Pierce, In situ diagnostics and prognostics of solder fatigue in IGBT modules for electric vehicle drives, IEEE Trans. Power Electron., vol. 30, no. 3, pp. 1535-1543, Mar. 2015.

[3] M. A. Khan, I. Husain, and Y. Sozer, Integrated electric motor drive and power electronics for bidirectional power flow between the electric vehicle and DC or AC grid, IEEE Trans. Power Electron., vol. 28, no. 12, pp. 5774-5783, Dec. 2013.

[4] O. C. Onar, J. Kobayashi, and A. Khaligh, A fully directional universal power electronic interface for EV, HEV, and PHEV applications, IEEE Trans. Power Electron., vol. 28, no. 12, pp. 5489-5498, Dec. 2013. [5] Y. S. Lai., W. T. Lee, Y. K. Lin, and J. F. Tsai, Integrated inverter/converter circuit and control technique of motor drives with dualmode control for EV/HEV applications, IEEE Trans. Power Electron., vol. 29, no. 3, pp. 1358-1365, Mar. 2014.

[6] P. Vithayasrichareon, G. Mills, and I. F. MacGill, Impact of electric vehicles and solar PV on future generation portfolio investment, IEEE Trans. Sustain. Energy., vol. 6, no. 3, pp. 899-908, Jul. 2015.

[7] D. G. Woo, D. M. Joo, and B. K. Lee, On the feasibility of integrated battery charger utilizing traction motor and inverter in plug-in hybrid electric vehicles, IEEE Trans. Power Electron., vol. 30, no. 12, pp. 7270- 7281, Dec. 2015.

[8] S. Dusmez, and A. Khaligh, A compact and integrated multifunctional power electronic interface for plug-in electric vehicles, IEEE Trans. Power Electron., vol. 28, no. 12, pp. 5690-5701, Dec. 2013.

[9] S. Rezaee, and E. Farjah, A DC-DC multiport module for integrating plug-In electric vehicles in a parking lot: topology and operation, IEEE Trans. Power Electron., vol. 29, no. 11, pp. 5688-5695, Nov. 2014.

[10] Q. Lei, D. Cao, and F. Z. Peng, Novel loss and harmonic minimized vector modulation for a current-fed quasi-Z-source

inverter in HEV motor drive application, IEEE Trans. Power Electron., vol. 29, no. 3, pp. 1344- 1357, Mar. 2014.

[11] L. Ni, D. J. Patterson, and J. L. Hudgins, High power current sensorless bidirectional 16-phase interleaved DC-DC converter for hybrid vehicle application, IEEE Trans. Power Electron., vol. 27, no. 3, pp. 1141-1151, Mar. 2012.